Evidence for an Influence of Local Dipole Excitations in Thermal Desorption

Luis G. Rosa, P. A. Jacobson, and P. A. Dowben*

Department of Physics and Astronomy, Behlen Laboratory of Physics, Center for Materials Research and Analysis, University of Nebraska−Lincoln, Lincoln, Nebraska 68588-0111

Received: August 31, 2005; In Final Form: February 28, 2006

Ferroelectric crystalline copolymer films of vinylidene fluoride with trifluoroethylene (70%:30%) strongly interact with the dipoles of adsorbed and absorbed water molecules. This interaction can be probed with laser-assisted thermal desorption techniques. The UV light enhancement of water desorption is strongly light polarization dependent. The electronic structure of the ferroelectric copolymer films of vinylidene fluoride with trifluoroethylene films is locally altered with incident UV radiation suggesting metastable excited states that may involve dipole reorientation.

Introduction

Surface dipole interactions have long been implicated as important in surface adsorption and surface catalysis.[1−3] The investigation of surface dipole interactions is, unfortunately, often complicated by the influence of the substrate including band structure effects[4] and strong perturbations due to surface charges inducing large surface dipoles at metal surfaces.[5] Ferroelectric materials provide a great opportunity to investigate dipole interactions with adsorbates, particularly as the surface electric dipoles are "reversible". Our preference for crystalline polymer ferroelectric materials[6,7] as a substrate for the study of adsorbate interactions with surface dipoles stems from the complex surfaces formed with the inorganic ferroelectric materials. The complexities associated with inorganic ferroelectrics include surface compositional instabilities, an abundance of lattice defects (point defects, steps, and grain boundaries), and considerable difficulty in preparing a stable reproducible surface with well-ordered dipoles oriented along the surface normal.

There is a growing body of evidence for dipole interactions between adsorbed water and ferroelectric crystalline copolymer films of vinylidene fluoride with trifluoroethylene P(VDF-TrFE 70%:30%). Both the formation of ice[8−10] on the surface and absorption[9−14] in ferroelectric crystalline copolymer films of vinylidene fluoride with trifluoroethylene (70%:30%) are known. Model calculations suggest that the formation of a hexagonal ice is influenced by the surface dipoles of P(VDF-TrFE).[8] In addition, water absorption is also seen to alter the dielectric properties of the ferroelectric crystalline copolymer films of vinylidene fluoride with trifluoroethylene (70%:30%).[11−14] Dipole interactions are also implicated by the observation that the ferroelectric transition in P(VDF-TrFE) has a profound effect on the absorption of water.[14] More compelling evidence for water−P(VDF-TrFE) dipole interactions is the suggestion of steric effects in thermal desorption[9] and attribution of the observed efficient H/D exchange between water and P(VDF-TrFE) to the large surface dipoles of P(VDF-TrFE).[10]

Surface dipoles can affect the binding site of water species adsorbed at the surface and sterically hinder or enhance the desorption of adsorbed and absorbed water. Here, we show that perturbations of local surface dipoles can affect desorption of absorbed water. The desorption of absorbed water is affected by the orientation of the electric vector potential of the incident UV light during the thermal desorption process, rather than simply the presence of UV illumination. These thermal desorption effects implicate dipole orientation within the ferroelectric or band symmetry selection rules (dipole selection rules) in a dipole related excitation. Consequently, either dipole rotational, or electronic excitations may play a significant role in the water interaction with the ferroelectric polymer surface.

Experimental Section

Ultrathin ferroelectric thin films of a copolymer of 70% vinylidene fluoride with 30% trifluoroethylene, P(VDF-TrFE 70:30), were fabricated by the Langmuir−Blodgett (LB) deposition technique on graphite substrates from the water subphase.[8−10] The P(VDF-TrFE 70:30) films, nominally some 3 to 7 molecular layers thick (15−35 Å thick, as noted) were prepared in ultrahigh vacuum by annealing at 110° C, which has proved to be an effective recipe in prior studies[6−10,15−20] and has been demonstrated to result in a surface free from impurities (including water).[15] For the experiments undertaken here, water vapor was exposed to the thin films of a copolymer of 70% vinylidene fluoride with 30% trifluoroethylene, P(VDF-TrFE 70:30) at 125 K.

The thermal desorption spectra were obtained by annealing the graphite substrate resistively, and exploiting our ability to make films of P(VDF-TrFE 70:30) sufficiently thin to obtain the necessary thermal conductivity through the ferroelectric polymer thin film. Water exposures are denoted in langmuirs where 1 L = 10^{-6} Torr·s with water exposed to P(VDF-TrFE) at 120 to 135 K. Laser-assisted thermal desorption, creating metastable excited states during thermal desorption, was undertaken. These experiments involved obtaining thermal desorption spectra while the surface was illuminated with a pulsed nitrogen gas laser (337 nm, 3.66 eV) at 20 Hz with an intensity of 100 kW/pulse (corresponding to 0.02 J/pulse). The incident 337 nm radiation was polarized by using a UV polarizer and focused onto the entire surface area of the sample (less than 2 cm^2). This corresponds to less than 20 photons per surface dipole per 200 ns pulse in the geometry of our experiment. In our experiments, we have compared linearly polarized light with the electric field vector **E** and the vector potential **A** of the incident radiation parallel with the surface to a polarization with

* Address correspondence to this author. Phone: 402-472-9838. Fax: 402-472-2879. E-mail: pdowben@unlinfo.unl.edu.

10.1021/jp054929n CCC: $30.25
Published on Web 03/28/2006

the electric field vector **E** and the vector potential **A** of the incident radiation perpendicular to the surface, but with the same radiation intensity/area and no change in light incidence angle. The desorbing species were collected normal to the film for both thermal desorption and photoassisted thermal desorption studies, unless stated otherwise. Because of the very low UV flux densities, we employed a very low heating rate. The heating rates for obtaining the thermal desorption spectra (TDS) were 0.5 deg/s throughout this work.

Inverse photoemission was undertaken by using a variable energy electron gun producing electron kinetic energies from 5 to 19 eV, incident normal to the surface. Photons were detected with a Geiger−Müller detector, as done in previous studies.[17−19] To create metastable excited states during inverse photoemission studies of P(VDF-TrFE), the sample was again illuminated with a pulsed nitrogen laser (337 nm, 3.66 eV) at 20 Hz with an intensity of 120 μJ/pulse, in the region of the incident electrons for inverse photoemission. This corresponds to about 1 photon per surface dipole per 4 ns pulse for the inverse photoemission experiments undertaken with UV light incident on the sample. Angle-resolved photoemission spectra were undertaken by using synchrotron radiation at a photon energy of 35 eV, dispersed by a 3 m toroidal grating monochromator, at the Center for Advanced Microstructure and Devices in Baton Rouge, LA.[20]

Evidence of Steric Effects in Thermal Desorption of Absorbed Water

For the most part, in this work we have made an effort to address adsorbed and absorbed water, not the adsorbed water ice that forms on the surface of P(VDF-TrFE).[8] Following exposure of water to crystalline thin films of P(VDF-TrFE) at 120−135 K, the thermal desorption spectra are largely characterized by two desorption peaks, as indicated in Figure 1, and reported elsewhere.[8−10] The desorption of water at 150−160 K is characteristic of water sublimation and this particular adsorption site does not saturate with increasing water exposure, but continues to increase in intensity. We associate this water species with the formation of surface "ice" or similar species. It is important to note that the formation of this ice-like species is not observed with small exposures of water to the P(VDF-TrFE) thin film samples cooled to 130 K. For P(VDF-TrFE) samples roughly 15 Å thick, more than 10 langmuirs are required for evidence of ice formation from thermal desorption, as seen in Figure 1a. For thicker films, greater exposures to water are required for the formation of ice, as determined in thermal desorption spectra,[8−10] and as indicated in Figure 1b for P(VDF-TrFE) samples roughly 35 Å thick.

The peak temperature, for the more strongly bound water species desorbing in the vicinity of 300 K and above, increases in temperature, the thicker the PVDF-TrFE film, as indicated in Figure 1, and discussed in detail elsewhere.[9] Because the desorption temperature of water from PVDF-TrFE above 280 K is associated with film thickness and water exposure, we associate this water species largely to absorbed water,[9] but a surface species cannot be completely excluded.[10]

For the thinner P(VDF-TrFE) samples roughly 15 Å thick, the thermal desorption spectra do provide an indication of a molecular water species at the surface that is significantly different from the absorbed water (Figure 1a). There is a thermal desorption feature at 280 to 320 K in addition to a thermal desorption feature that begins at about 350 K, as seen in Figure 1a. As the P(VDF-TrFE) sample thickness increases, the water thermal desorption feature at 280 to 320 K is increasingly difficult to observe, and we can propose several reasons for these

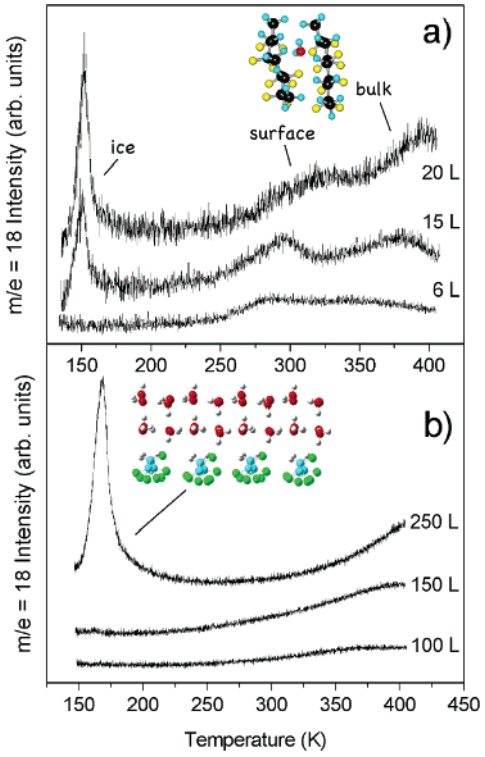

Figure 1. Thermal desorption spectra (TDS) of water from a thin (15 Å thick) P(VDF-TrFE 70:30) on graphite for 6, 15, and 20 L of exposure to water at 130 K (1 L = 1 × 10^{-6} Torr•s) is shown (a). Thermal desorption spectra (TDS) of water from a thicker (35 Å thick) P(VDF-TrFE 70:30) on graphite for 100, 150, and 250 L of exposure to water at 130 K (1 L = 1 × 10^{-6} Torr•s) is shown (b). The assignment of the thermal desorption features to water ice (150 K) and absorbed water in P(VDF-TrFE) (300 K) is indicated by the schematic minimum energy structures in panel a, with the adsorbed surface water likely contributing to the thermal desorption feature at about 300 K in panel a and absorbed water contributing to the thermal desorption of water at even high temperatures (see text).

difficulties. While the existence of an adsorbed surface water species distinct from an absorbed water species is indicated in simple model calculations,[10] with increasing P(VDF-TrFE) sample thickness, the volume for absorbed water increases and the water absorption site (water in the bulk of the film) may well be much more energetically favorable than surface water adsorption sites.[10] Alternatively, with increasing P(VDF-TrFE) sample thickness, the high degree of in-plane (lateral) surface order observed with the thinner films[16] is lost or reduced. In addition, at the very high concentrations of absorbed water, following very large water exposures to P(VDF-TrFE) at 130 K, small amounts of water desorption from surface sites will be easily obscured by background and the thermal desorption signals from adsorbed water, as indicated in Figure 1b. High concentrations of absorbed water may be an essential ingredient to observing the water thermal desorption feature at 280−320 K. This water thermal desorption feature at 280−320 K, observed with very thin (15 Å) P(VDF-TrFE) films, has an angular dependence that also suggests a surface origin.[9]

For the thermal desorption of water that occurs in the vicinity of 280−320 K, that is to say the desorption of water not related to a surface water ice on P(VDF-TrFE), the desorption of water in an off-normal direction may be enhanced. This appears particularly true for very thin films of P(VDF-TrFE). Angle-resolved thermal desorption was undertaken at various take-off angles ranging from 0° to 65° with respect to the film surface normal. The angle-resolved thermal desorption studies were

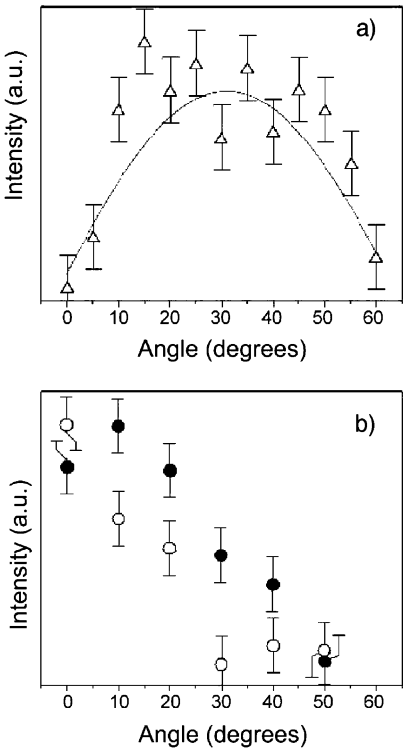

Figure 2. The integrated intensity of water desorbing from P(VDF-TrFE) as a function of angle with respect to the surface normal is shown following 5 langmuirs of water exposure to (a) 15 (△) and (b) 25 Å thick (●) P(VDF-TrFE) thin films at 130 K. In panel b the integrated intensity of water desorbing from PVDF-TrFE as a function of angle, enhanced by illumination with 337 nm UV radiation plane polarized to place **E** in the plane of the film and following 5 langmuirs of water exposure to 25 Å thick PVDF-TrFE thin films at 130 K is also plotted (○). The $\sin^2$ curve in panel a is meant only to guide the eye.

undertaken with the thinner films (about 15 and 25 Å thick) and with the smaller water exposures to avoid any complications of ice formation. The desorbing water species, following 5 langmuirs of water exposure to 15 Å P(VDF-TrFE) films at 120 K, is attributed solely to the absorbed water species (where the thermal desorption occurs in the vicinity of 280−300 K) not the surface "ice" thermal desorption feature appearing at 150−160 K. For the thinner 15 Å thick P(VDF-TrFE) films (with a larger polymer surface-to-volume ratio), the water thermal desorption intensity is peaked at 30° off normal, strong evidence of steric or geometric effects.[9] The intensity of the integrated water thermal desorption peak, in the vicinity of 280−300 K (the most significant water thermal desorption peak at this water exposure), is plotted in Figure 2a, indicating a preference for water desorption off-normal. For the slightly thicker 25 Å thick P(VDF-TrFE) films, the preference for off-normal thermal desorption of water is lost, and the normalized water desorption intensity is peaked near 0°, i.e., desorption is more favorable in a direction close to the surface normal (Figure 2b). Indeed, even for the thinner 15 Å thick P(VDF-TrFE) films (with a larger polymer surface-to-volume ratio), there is little or no preference for off-normal desorption in the water thermal desorption intensity for the water thermal desorption feature beginning at about 350 K. This too is consistent with an adsorbed surface water species distinct from an absorbed water species, as proposed elsewhere.[10]

The enhancement of water desorption in an off-normal direction for the thinner P(VDF-TrFE) films (Figure 2a) is a further experimental indication of a molecular water species at the surface (or near-surface region) of P(VDF-TrFE) that is

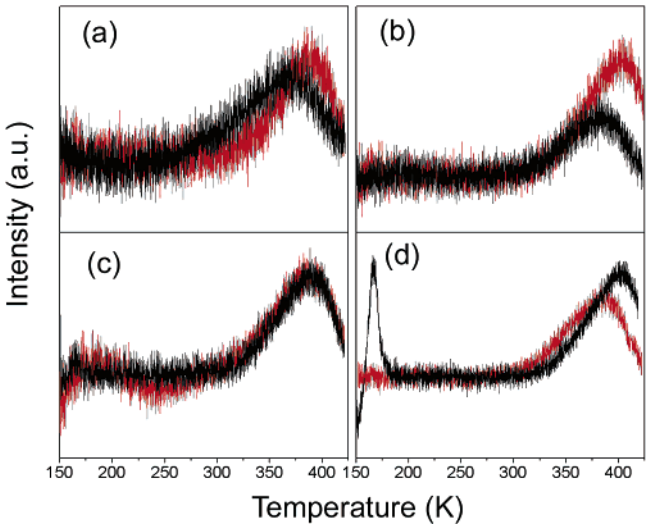

Figure 3. Laser-assisted thermal desorption for (a) 200, (b) 250, (c) 300, and (d) 350 langmuirs of water exposure. The experiments were undertaken with incident light polarized with **E** parallel with film surface (black) and **E** parallel with the surface normal (red). Desorption of water was measured along the surface normal.

distinct from the absorbed water and surface ice or there is a portion of the desorbing absorbed water species sensitive to the surface structure. With either interpretation, these angle-resolved thermal desorption studies suggest that surface dipole orientation matters in the thermal desorption of absorbed water in this system. At issue is whether there is more direct evidence of an interaction between the surface dipole and the desorption of water.

Laser-Assisted Thermal Desorption of Absorbed Water in P(VDF-TrFE)

Although a somewhat unusual surface spectroscopy technique, evidence for the influence of either dipole interactions or the preferential orientation of an adsorbed water species can be found in laser-assisted thermal desorption. As seen in Figure 3, the thermal desorption of water is seen to be dependent on the light polarization of the incident radiation on the P(VDF-TrFE).

Easily identified is the affect of the light polarization on the laser-assisted thermal desorption of absorbed water in P(VDF-TrFE), with the desorption temperature of 300−400 K. With **E** of the incident light parallel with the surface, the thermal desorption of absorbed water is promoted for smaller water exposures (200 to 250 L) to a 35 Å P(VDF-TrFE) thick film at 120−135 K. The light-enhanced thermal desorption of absorbed water occurs at a lower temperature with the incident light **E** parallel with the surface when compared with light-enhanced thermal desorption of water undertaken with the **E** of the incident light parallel with the surface normal. At higher water exposures this effect is lost (Figure 3c,d). Since the UV laser light intensity is unaltered in these experiments, and only the light polarization is changed, light polarization is clearly an important factor.

There is some further evidence that either the water dipole orientation or the dipoles of the P(VDF-TrFE) surface play a role in the laser-assisted thermal desorption of adsorbed or absorbed water. As seen in Figure 2b, a preference for the absorbed water species to desorb more normal to the surface is enhanced when angle resolved thermal desorption, from the 25 Å thick P(VDF-TrFE) sample, is undertaken with illumination. In this experiment (Figure 2b), the incident light is polarized with **E** parallel with the surface. Certainly, UV light illumination

removes any residual steric (enhanced off normal) effects from the thermal desorption process and tends to restore the expected $\cos^{\beta}\theta$ distribution.[21] This behavior also suggests that illumination with UV radiation, polarized with the **E** parallel with the surface, enhances the thermal desorption of absorbed water from P(VDF-TrFE).

The enhancement of absorbed/adsorbed water desorption with illumination from UV light, polarized with **E** parallel with the surface, is not a direct result of a pyroelectric effect[7,22] as the thermal desorption geometry and photon flux is the same for both light polarizations for the data plotted in Figure 3. Rather, electronic excitations are implicated in the light enhancement of the thermal desorption of water. The light polarization dependence does not just completely exclude pyroelectric effects as a source of the enhancement of water thermal desorption, but does suggest that the electronic excitations are band or state symmetry dependent.

Changes in the light polarization dependence of UV light-enhanced thermal desorption of absorbed water from P(VDF-TrFE) with the amount of water absorption suggests that the local symmetry of (PVDF-TrFE) plays a significant role. The enhancement of the UV laser-assisted desorption of absorbed water from P(VDF-TrFE) with **E** parallel with the surface occurs at low absorbed water concentrations (Figure 3a,b), where the high local C_{2v} point group symmetry of P(VDF) is preserved.[20,23] At high concentrations of absorbed water in P(VDF-TrFE), the enhancement of the laser-assisted desorption of absorbed water from P(VDF-TrFE) occurs with the UV laser light polarized with **E** parallel with the surface normal (Figure 3d). Water absorption does create distortions of the P(VDF-TrFE) chains leading to a reduction of crystallinity[11] and a distortion of the dipoles away from the surface normal in the immediate proximity of the water molecule,[10] so a significant reduction in local point group symmetry is expected with large concentrations of absorbed water.

Light polarization effects in the laser-assisted thermal desorption experiments are dependent upon the absorbed water content in the film. This provides clear evidence that the effects, seen in Figure 3, are not simply the result of a difference in the light absorbance by the sample due to changes in polarization alone (as boundary conditions, i.e., as Fresnel's equations, might suggest). From Fresnel's equations alone, the reflectivity should be highest, and the adsorption lowest with **E** parallel with the surface, in the geometry of our experiment. This geometry, with **E** parallel with the surface, is exactly when the greatest laser enhancement of the thermal desorption process occurs (Figure 3a). If laser-assisted thermal desorption were simply a function of the light absorption due to boundary conditions at the dielectric interface, then the laser-assisted thermal desorption should be enhanced with **E** parallel with the surface normal, and this is not the case except when the absorbed water content is (relatively) high.

While suggested by other studies,[14] we can exclude the well-known P(VDF-TrFE, 70%:30%) ferroelectric to paraelectric phase transition at 80° C[7,8,19] as being the sole cause of the enhanced thermal desorption of water from P(VDF-TrFE). For small water exposures to P(VDF-TrFE) at 125 K, the light-enhanced thermal desorption of absorbed water will begin to occur at temperatures below 350 K, as seen in Figure 3. The surface phase transition at 20 °C,[6−7,15−20] however, cannot be easily excluded from playing a role in the thermal desorption process. The possible structural dipole reorientations[16−20] that accompany this phase transition occur near the temperature range of absorbed water thermal desorption and may be enhanced by UV light. Such effects are difficult to disentangle from the consequences of single dipole reorientation events. Either way, dipole reorientation is a leading candidate for explaining the light polarization-dependent enhancement of absorbed water thermal desorption from P(VDF-TrFE).

With 20 photons per surface dipole per pulse, multiphoton excitation effects can be excluded for several reasons. Our strongest reason for excluding multiphoton effects is that the power dependence on the laser-assisted thermal desorption appears to be very weak over the range of 10−25 photons per surface dipole per pulse. In addition, at this photon flux density, the absorption cross-section for 337 nm radiation in a 25 Å thick P(VDF-TrFE) film would have to be very high. Both ice and P(VDF-TrFE) are transparent for visible and near-UV photons. States would have to be available within the highest occupied molecular orbital (HOMO) to lowest unoccupied molecular orbital (LUMO) gap of either water or P(VDF-TrFE). As discussed below, the HOMO-LUMO gaps for both molecules are significant. This and the significant reflectivity of the (substrate) sample, in the geometry of our experiment, suggests that the absorption cross-section is not large enough for multiphoton events to be very likely at the photon flux densities of this experiment in P(VDF-TrFE), with absorbed water.

UV radiation damage to the sample[24] is also unlikely to be the cause of polarization-dependent laser-assisted thermal desorption effects observed here. The P(VDF-TrFE) polymer thin films, used in the experiments throughout this work, appear robust with respect to radiation. The water thermal desorption spectra and characteristic photoemission and inverse photoemission spectra of P(VDF-TrFE) appear identical with the pristine films after an extensive number of UV light-enhanced thermal desorption experiments (i.e., the water thermal desorption returns to "normal" after the UV experiments). This does not exclude radiation damage,[15,24] but does clearly indicate that such damage is not significant enough to alter the water thermal desorption spectra by itself.

The fact that the laser-assisted thermal desorption of water does occur at a lower temperature (Figure 3) than is the case in the absence of illumination (Figure 1b) suggests that laser heating effects may play a role in the desorption of absorbed water, but light-assisted thermal desorption of ice, as discussed below, and the light polarization-dependence noted above provide considerable evidence that this effect is not significant, and certainly not the complete explanation for the laser enhance thermal desorption effect observed.

Laser-Stimulated Thermal Desorption of Water Ice on P(VDF-TrFE)

Although not the major emphasis of this effort, it seems worth noting in passing that the desorption of water ice from P(VDF-TrFE) is also significantly affected by incident UV light. The water thermal desorption spectra taken in the absence of laser illumination (Figure 1b) make it clear that there exists evidence of water ice in thermal desorption spectra following 200 langmuirs or more water exposure to 35 Å thick P(VDF-TrFE) films at 130 K. This characteristic signature of water ice formation, in the thermal desorption spectra, is absent in the laser-assisted thermal desorption spectra taken following 200, 250, and 300 L water exposure to 35 Å thick P(VDF-TrFE) films at 130 K, as seen in Figure 3, with the incident light **E** parallel with the surface and with the **E** of the incident light parallel with the surface normal. This comparison of the water thermal desorption spectra taken in the absence of laser illumination (Figure 1b) and in the presence of laser illumination (Figure 3) indicates that there is a significant amount of water

ice desorbing almost immediately when the P(VDF-TrFE) is illuminated with UV light.

In the laser-assisted thermal desorption spectra taken following 350 L water exposure to 35 Å thick P(VDF-TrFE) films at 130 K, as seen in Figure 3d, there are some residual features due to the thermal desorption attributable to ice with **E** parallel with the surface (the thermal desorption of water observed at 150−160 K) but not with the incident light polarized so that **E** is parallel with the surface normal. Thus the light-assisted thermal desorption of water ice is further enhanced when the incident light polarized so that **E** is parallel with the surface normal. This effect could, however, be a result of enhanced light absorption with this light polarization (**E** is parallel with the surface normal), as boundary conditions, i.e., as Fresnel's equations, might suggest (as noted above). The presence of the water ice thermal desorption feature in Figure 3d does tend, however, to suggest the desorption of water ice is not caused by substrate heating with the UV light illumination (or else the thermal desorption feature would be much shifted in temperature).

Given that the surface ice formed on P(VDF-TrFE) can be many layers thick and that the highest occupied molecular orbital to lowest unoccupied molecular orbital gap for water ice is more that 13 eV,[8] this enhanced thermal desorption process is also unlikely to be a multiphoton process. More importantly, these light polarization effects in the UV light stimulated thermal desorption of water ice at 150−160 K tend to exclude both the well-known film ferroelectric to paraelectric transition at 80° C[7,8,19] and the surface phase transition at 20 °C[6−7,15−20] as the sole cause of light-enhanced thermal desorption. The water ice does adopt an interface structure that does have some registry with the surface P(VDF-TrFE) dipoles, so alteration of the underlying P(VDF-TrFE) dipole could influence the surface water ice, as has been suggested previously.[8]

UV radiation enhanced thermal desorption of water from ice is not entirely unexpected, even in the presence of P(VDF-TrFE). Laser-stimulated changes to the microstructure of water ice, as a result of nonthermal UV radiation, and the concomitant changes to the thermal desorption of ice have been reported.[25] Photoexcited carriers to defect states in ice, from the underlying graphite substrate, were suggested as the origin for the laser-stimulated changes to the microstructure of water ice.[25] With an ice layer, our system resembles a trilayer system: water ice on P(VDF-TrFE) with absorbed water on graphite and boundary conditions cannot be excluded (i.e., Fresnel's equations, as just noted). In this latter system, the origin of the UV light-enhanced thermal desorption is difficult to identify uniquely, but the photoexcitation of carriers from the graphite to the P(VDF-TrFE) or water absorbed in P(VDF-TrFE) is certainly possible, as discussed below. As a result, the desorption of water ice could be enhanced by dipole reorientation of the underlying P(VDF-TrFE), dipole reorientation in the water ice, or Coulombic repulsion due to charge buildup (due to charge excitations) in the adsorbed water ice, in the presence of the UV laser illumination.

Laser-Induced Changes in Electronic Structure

As seen in Figure 4, the combined photoemission and inverse photoemission spectra of P(VDF-TrFE) are consistent with a wide band gap insulator and theoretical expectations. With hydrogen terminated (to prevent excessive folding), semiempirical molecular orbital calculations undertaken by PM3-NDO (neglect of differential overlap) with the HyperChem package of short chain lengths of P(VDF-TrFE) have recovered much

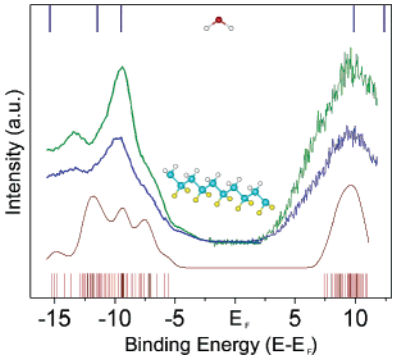

Figure 4. Combined photoemission and inverse photoemission of P(VDF-TrFE) thin films (15−20 Å thick) on graphite (green) are compared to P(VDF-TrFE) following exposure to 200 langmuirs of water at 190 K (blue). For reference, a calculated density of states (DOS) of PVDF is shown, obtained by applying equal Gaussian envelopes of 1 eV full width half-maximum to each molecular orbital (shown at the bottom), to account for the solid-state broadening in photoemission, and then summing. The calculated electronic states of water are at the top of the panel.

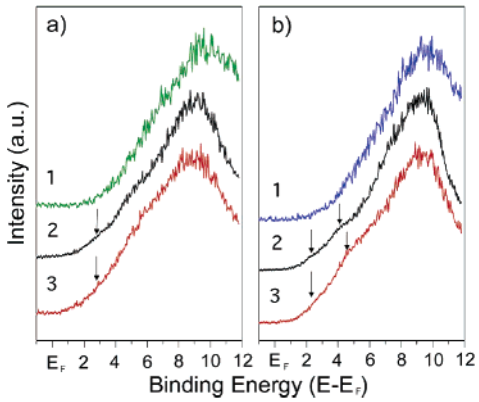

Figure 5. Inverse photoemission of clean P(VDF-TrFE) (green, curve 1) (in panel a) and with water (blue, curve 1) (in panel b). Inverse photoemission of unoccupied states with the excitation of metastable states of clean PVDF (a) and following 100 langmuirs of water exposure at 190 K (b). The experiments were undertaken with incident UV laser light (337 nm) polarized with **E** parallel to the film surface (black, curves 2) and parallel to the surface normal (red, curves 3). The molecular (PVDF-TrFE) film is 20−25 Å thick. The arrows in the figure indicate some of the regions of apparent added unoccupied density of states with UV irradiation.

of the detail observed in the combined photoemission and inverse photoemission, as has been noted with other polymers[26] and large adsorbed molecular system[27] experimental and semiempirical theory comparisons. The absorption of water diminishes the photoemission and inverse photoemission intensities associated with P(VDF-TrFE) and leads to an increase in the width of the P(VDF-TrFE) photoemission and inverse photoemission features, as seen in Figure 4. Strong alterations of the observed P(VDF-TrFE) electronic structure are not observed with water absorption. It is under the illumination of UV radiation that changes in the density of states are observed at the conduction band edge.

As seen in Figure 5, the illumination of 337 nm (3.66 eV) light on the ferroelectric P(VDF-TrFE) thin films induces a small increase in the density of states at the conduction band edge. With UV irradiation the unoccupied density of states moves closer to the Fermi level as observed in inverse photoemission (Figure 4a). With the absorption of water, the increase in the unoccupied density of states near the Fermi level is even more pronounced in inverse photoemission (Figure 5b). We cannot

yet conclusively assign the origin of the increase in the unoccupied density of states near the Fermi level due to UV irradiation. With about 1 photon per surface dipole per 4 ns pulse in the geometry of our inverse photoemission experiment, the fact that any change is observed in the inverse photoemission spectra with illumination is quite surprising. From scanning tunneling microscopy telegraph noise, we estimate the single dipole switching (or single dipole excitation) in this system occurs on the scale of 1 ns. The observation of a change in the density of states (however small), with sample illumination of the sample with a pulsed nitrogen laser (337 nm, 3.66 eV) at 20 Hz with an intensity of 120 μJ/pulse strongly suggests the excitation of long-lived metastable states.

We have seen that the conduction (unoccupied) band edge does shift closer to the Fermi level and the band structure changes dramatically as the temperature is increased across the surface ferroelectric transition phase of P(VDF-TrFE) at about 295 K[6−7,17−19] (distinct from the bulk ferroelectric transition at about 350 K[7,8,19]). The increase in the apparent density of unoccupied states near the Fermi level, observed here, is far less than that observed across the surface ferroelectric phase transition at about 295 K.[17−19] This is expected as the temperature for the inverse photoemission measurements here (190 K) is well below the surface ferroelectric phase transition while the UV flux/area is insufficient to alter more than a small fraction of the surface dipoles unless the excited states are extremely long lived. To prevent the formation of an ice layer, these inverse photoemission studies were undertaken at temperatures above a P(VDF-TrFE) compressibility (lattice stiffening) at about 160 K,[20,28] at temperatures where electron−phonon coupling has been implicated,[20,23,28] and this could affect the activation barrier to dipole reorientation.

The fact that there is a greater increase in the unoccupied density of states near the Fermi level under UV illumination with absorbed water than without is consistent with a more facile local dipole reorientation in P(VDF-TrFE) when water is present, and very long-lived metastable states that involve dipole reorientation. Again, water absorption does create distortions of the P(VDF-TrFE) chains leading to a reduction of crystallinity[11] and a distortion of the ferroelectric dipoles away from the surface normal in the immediate proximity to the water molecule.[10] This could also lower the activation barrier to dipole reversal (or just a significant dipole or multiple dipole reorientation) with electronic or dipole excitations. The long lifetime suggests that multiple dipoles may "switch" with a single electron excitation, and this is consistent with steric hindrance (structural complexities) for single dipole reorientation.

We believe that either change in the dipole orientation or the changes in electronic structure caused by UV irradiation-induced excitations enhances the desorption of water from the surface of P(VDF-TrFE). The cross section for the absorption of UV radiation by both P(VDF-TrFE)[29] and water[30] is low. So as noted above, the likely mechanism for both the change in the density of states and the polarization-dependent light-stimulated thermal desorption of absorbed water is electron (carrier) excitation from the graphite substrate accompanied by a metastable dipole reorientation of the polymer. We know from scanning tunneling microscopy studies that changing the applied bias will alter the dipole orientation,[16] and from scanning tunneling microscopy studies, we believe that charge attachment may well lead to the long-lived state with dipole reorientation(s).

The 3.66 eV photon energy is more than enough to excite electrons into the unoccupied states of P(VDF-TrFE) or H_2O from the Fermi level of graphite; such excitations from a conducting substrate to a molecular adsorbate are predicted for CO on Pt(111)[31] and water on graphite,[25] for example. Photodesorption of CO_2 and H_2O from oxide semiconductors due to UV light-induced band gap excitations have been reported.[32−33] UV light-induced photoisomerization, likely due to exciton formation or an isolated carrier excitation, are known in other systems.[34] This latter photoisomerization from *trans*-stilbene and *cis*-stilbene[34] is similar to the transition from the all-trans configuration of ferroelectric P(VDF-TrFE).

Summary

It is likely that changes in local dipole orientation and the formation of long-lived metastable states affect the heat of adsorption and desorption. The photoexcitation and subsequent electron attachment to water to form H_2O^- or $[-CH_2-CF_2-]^-$ may also occur, though energy considerations make this unlikely for the absorbed water directly. As already noted, such electron attachment has been suggested to cause molecular reorientation in water ice on graphite.[25] Model calculations suggest that the surface dipoles of the ferroelectric P(VDF-TrFE) induce preferential orientations for adsorbed and absorbed water.[10] This should not be too surprising as water has been identified as a cause of reorientation at polymer surfaces,[35−38] including the surface structure of fluorinated polymers.[39−41]

Light polarization-dependent photoassisted thermal desorption has now been demonstrated as a method for excitation symmetry effects on adsorbate interactions and possibly different preferential adsorbate and substrate molecular orientations.

Acknowledgment. This work was supported by the National Science Foundation through grant CHE-0415421. The authors are grateful to S. Ducharme, C. Othon, and M. Poulsen for access to their sample fabrication facilities, and to Jie Xiao for his technical assistance and contributions.

References and Notes

(1) Whitman, L. J.; Bartosch, C. E.; Ho, W.; Strasser, G.; Grunze, M. *Phys. Rev. Lett.* **1986**, *56*, 1984. Whitman, L. J.; Bartosch, C. E.; Ho, W. *J. Chem. Phys.* **1986**, *85*, 3688.

(2) Ertl, G.; Lee, S. B.; Weiss, M. *Surf. Sci.* **1982**, *114*, 527.

(3) Kiskinova, M.; Goodman, D. W. *Surf. Sci.* **1981**, *108*, 64.

(4) Dowben, P. A.; Miller, A.; Ruppender, H.-J.; Grunze, M. *Surf. Sci.* **1988**, *193*, 336.

(5) Nørskov, J. K.; Holloway, S.; Lang, N. D. *Surf. Sci.* **1984**, *137*, 65.

(6) Blinov, L. M.; Fridkin, V. M.; Palto, S. P.; Bune, A. V.; Dowben, P. A.; Ducharme, S. *Usp. Fiz. Nauk* **2000**, *170*, 247−262; *Phys.-Usp.* (*Engl. Transl.*) **2000**, *43*, 243−257.

(7) Ducharme, S.; Palto, S. P.; Fridkin, V. M. Ferroelectric Polymer Langmuir−Blodgett Films. In *Handbook of Surfaces and Interfaces of Materials, Ferroelectric and Dielectric Films*; Academic: San Diego, CA, 2002, Vol. 3, pp 546−592.

(8) Rosa, L. G.; Xiao, J.; Losovyj, Ya. B.; Gao, Y.; Yakovkin, I. N.; Zeng, X. C.; Dowben, P. A. *J. Am. Chem. Soc*. **2005**, *127*, 17261.

(9) Rosa, L. G.; Jacobson, P. A.; Dowben, P. A. *J. Phys. Chem. B* **2005**, *109*, 532−535.

(10) Rosa, L. G.; Yakovkin, I. N.; Dowben, P. A. *J. Phys. Chem. B* **2005**, *109*, 14189−14197.

(11) Jacobson, P. A.; Rosa, L. G.; Othon, C. M.; Kraemer, K.; Sorokin, A. V.; Ducharme, S.; Dowben, P. A. *Appl. Phys. Lett.* **2004**, *84*, 88−90.

(12) Castela, A. S.; Simoes, A. M. *Corros. Sci.* **2003**, *45*, 1631.

(13) Castela, A. S.; Simoes, A. M. *Corros. Sci.* **2002**, *45*, 1647.

(14) Levshin, N. L.; Yudin, S. G.; Diankina, A. P. *Moscow Univ. Phys. Bull.* **1997**, *52*, 71−74. Levshin, N. L.; Yudin, S. G. *Vysokomol. Soedin., Ser. B* **2004**, *46*, 1981 (Engl. Transl.). Levshin, N. L.; Yudin, S. G. *Polym. Sci. Ser. B* **2004**, *46*, 348.

(15) Choi, J.; Morikawa, E.; Ducharme, S.; Dowben, P. A. *Matt. Lett.* **2005**, *59*, 3599−3603.

(16) Qu, H.; Yao, W.; Garcia, T.; Zhang, J.; Sorokin, A. V.; Ducharme, S.; Dowben, P. A.; Fridkin, V. M. *Appl. Phys. Lett.* **2003**, *82*, 4322. Cai,

L.; Qu, H.; Lu, C.; Ducharme, S.; Dowben, P. A.; Zhang, J. *Phys. Rev. B* **2004**, *70*, 155411.

(17) Choi, J.; Dowben, P. A.; Pebley, S.; Bune, A.; Ducharme, S.; Fridkin, V. M.; Palto, S. P.; Petukhova, N. *Phys. Rev. Lett.* **1998**, *80*, 1328−1331.

(18) Choi, J.; Dowben, P. A.; Ducharme, S.; Fridkin, V. M.; Palto, S. P.; Petukhova, N.; Yudin, S. G. *Phys. Lett. A* **1998**, *249*, 505−511.

(19) Choi, J.; Borca, C. N.; Dowben, P. A.; Bune, A.; Poulsen, M.; Pebley, S.; Adenwalla, S.; Ducharme, S.; Robertson, L.; Fridkin, V. M.; Palto, S. P.; Petukhova, N.; Sorokin, A. V. *Phys. Rev. B* **2000**, *61*, 5760−5770.

(20) Choi, J.; Tang, S.-J.; Sprunger, P. T.; Dowben, P. A.; Fridkin, V. M.; Sorokin, A. V.; Palto, S. P.; Petukhova, N.; Yudin, S. G. *J. Phys. Condens. Matter* **2000**, *12*, 4735−4745.

(21) Willigen, W. *Phys. Lett.* **1968**, *28A*, 80. Polanyi, J. C.; Wong, W. H. *J. Chem. Phys.* **1969**, *51*, 1439. Steinrück, H. P.; Winkler, A.; Rendulic, K. D. *J. Phys. C* **1984**, *17*, L311. Steinrück, H. P.; Luger, M.; Winkler, A.; Rendulic, K. D. *Phys. Rev. B* **1985**, *32*, 5032. Steinrück, H. P.; Winkler, A.; Rendulic, K. D. *Surf. Sci.* **1985**, *154*, 99. Steinrück, H. P.; Winkler, A.; Rendulic, K. D. *Surf. Sci.* **1985**, *152*/*153*, 323.

(22) Chynoweth, A. G. *J. Appl. Phys.* **1956**, *27*, 78. Peterson, B. W.; Ducharme, S.; Fridkin, V. M.; Reece, T. J. *Ferroelectrics* **2004**, *304*, 51−54. Ducharme, S.; Bai, M.; Poulsen, M.; Adenwalla, S.; Palto, S. P.; Blinov, L. M.; Fridkin, V. M. *Ferroelectrics* **2001**, *252*, 191.

(23) Rosa, L. G.; Losovyj, Ya. B.; Choi, J.; Dowben, P. A. *J. Phys. Chem. B* **2005**, *109*, 7817−7820.

(24) Choi, J.; Manohara, H. M.; Morikawa, E.; Sprunger, P. T.; Dowben, P. A.; Palto, S. P. *Appl. Phys. Lett.* **2000**, *76*, 381−383. Manohara, H. M.; Morikawa, E.; Choi, J.; Sprunger, P. T. *IEEE J. Microelectromech. Syst.* **1999**, *8*, 417−423. Morikawa, E.; Choi, J.; Manohara, H. M.; Ishii, H.; Seki, K.; Okudaira, K. K.; Ueno, N. *J. Appl. Phys.* **2000**, *87*, 4010−4016.

(25) Charkarov, D.; Kasemo, B. *Phys. Rev. Lett.* **1998**, *81*, 5181.

(26) Chambers, D. K.; Karanam, S.; Qi, D.; Selmic, S.; Losovyj, Ya. B.; Rosa, L. G.; Dowben, P. A. *Appl. Phys. A* **2005**, *80*, 483−488. Feng, D.-Q.; Caruso, A. N.; Schulz, D. L.; Losovyj, Ya. B.; Dowben, P. A. *J. Phys. Chem. B* **2005**, *109*, 16382−16389.

(27) Caruso, A. N.; Bernard, L.; Xu, B.; Dowben, P. A. *J. Phys. Chem. B* **2003**, *107*, 9620−9623. Caruso, A. N.; Rajesh, R.; Gallup, G.; Redepenning, J.; Dowben, P. A. *J. Phys. Chem. B* **2004**, *108*, 6910−6914. Caruso, A. N.; Rajesekaran, R.; Gallup, G.; Redepenning, J.; Dowben, P. A. *J. Phys. Condens. Matter* **2004**, *16*, 845−860. Kahn, A.; Cornil, J.; dos. Santos, D. A.; Brédas, J. L. *Chem. Phys. Lett.* **2000**, *317*, 444.

(28) Borca, C. N.; Adenwalla, S.; Choi, J.; Sprunger, P. T.; Ducharme, S.; Robertson, L.; Palto, S. P.; Liu, J.; Poulsen, M.; Fridkin, V. M.; You, H.; Dowben, P. A. *Phys. Rev. Lett.* **1999**, *83*, 4562−4565.

(29) Bai, M.; Sorokin, A. V.; Thompson, D. W.; Poulsen, M.; Ducharme, S.; Herzinger, C. M.; Palto, S.; Fridkin, V. M.; Yudin, S. G.; Savchenko, V. E.; Gribova, L. K. *J. Appl. Phys.* **2004**, *95*, 3372.

(30) Kobayashi, K. *J. Phys. Chem.* **1983**, *87*, 4317.

(31) Besley, N. A. *J. Chem. Phys.* **2005**, *122*, 184706.

(32) Kawai, T.; Sakata, T. *Chem. Phys. Lett.* **1980**, *69*, 33−36.

(33) van Hieu, N.; Lichtman, D. *Surf. Sci.* **1981**, *103*, 535−541.

(34) Tsai, C.-S.; Wang, J.-K.; Skodje, R. T.; Lin, J.-C. *J. Am. Chem. Soc.* **2005**, *127*, 10788−10789.

(35) Yasuda, T.; Miyyama, M.; Yasuda, H. *Langmuir* **1994**, *10*, 583.

(36) Hawkridge, A. M.; Gardella, J. A., Jr.; Toselli, M. *Macromolecules* **2002**, *35*, 6533.

(37) Lee, S. H.; Ruckenstein, E. *J. Colloid Interface Sci.* **1987**, *120*, 529.

(38) Lukás, J.; Sodhi, R. N. S.; Sefton, M. V. *J. Colloid Interface Sci.* **1995**, *174*, 421.

(39) Yasuda, H.; Okuno, T.; Sawa, Y. *Langnuir* **1995**, *11*, 3255.

(40) Ruckenstein, E.; Gourisankar, S. V. *J. Colloid Interface Sci.* **1985**, *107*, 488.

(41) Ruckenstein, E.; Gourisankar, S. V. *J. Colloid Interface Sci.* **1986**, *109*, 557.